

CHAPTER II

THEORY

II.1 Out line of Reaction Mechanism :

The mechanism of interaction between nucleons and nuclei is not exactly describable due to the lack of exact knowledge of the law of nuclear forces. Hence the problem of nucleon-nucleus interaction or in other words, reaction mechanism, has been attacked from different approaches so as to arrive at a reasonable theoretical understanding of the experimentally observed facts. Basically there exist two different approaches: one that can be called “Black Box” or “Model” approach, the other that can be connected in some way to the many-body methods used in nuclear physics.

In the model approach, a simple mathematically solvable model is proposed, guided by the experimental observables. In this approach, obviously the dynamics of the nuclear many-body system is dismissed as, impossible to handle. The compound nucleus model, direct reaction model and the optical model fall into this category. These models yield expressions for the cross sections, polarisation and angular distributions without really solving the complete dynamical problem. In the second approach, the many-body methods used in nuclear structure studies are essentially extended to the problem of nuclear reactions, based on the idea that the unbound continuous states of the collision problem can be treated analogously to the bound levels of the nucleons in the atomic nucleus. The obvious difficulty in solving nuclear many-body problems which is well beyond the contemporary theoretical development is responsible for its application only to a limited class of nuclear phenomena. As is evident from the literature, bulk of our knowledge about the mechanism of interaction comes from the model approach.

Two extreme models of nuclear reactions have received particular attention for a long time and enjoyed commensurate success. They are the direct reaction

model and the compound nucleus model. The fast direct reactions are supposed to be initiated and completed at the very first projectile target collision and hence they occur within the time ($\sim 10^{-22}$ sec) taken by the projectile to cross the nuclear diameter. On the other hand, the slow compound nuclear reaction continues to the end of a very large number of internal collisions and therefore takes a comparatively long time ($\sim 10^{-15}$ sec). Although these times of interaction can not be measured experimentally, the two types of reactions can be distinguished by various experimental features. For example, the outgoing particles of the compound nuclear reaction show a continuous Maxwellian distribution in their energies whereas those emitted in direct reactions have discrete energies characteristic of the residual nucleus. Secondly, the angular distribution of the emitted particles in compound nuclear reactions is characterised by fore and aft symmetry (symmetry around 90°) whereas it is predominantly forward-peaked in direct reactions. A third distinction lies in that the emitted particles are partially polarised in direct reactions whereas they are completely unpolarised in compound nuclear reactions. However in recent years, there has been an increasing evidence pointing out to new types of process that occur with intermediate time scales between 10^{-16} to 10^{-21} sec. These are indicated by the unexpected shape of the excitation functions, non-Maxwellian energy distribution and forward-peaked angular distribution of the emitted particles. The newly observed processes are called "preequilibrium" or "precompound" reactions, as they occur in time sequence prior to the establishment of the equilibrium compound nucleus stage.

In what follows, a brief description of the traditional direct and compound nucleus reactions will be first given followed by a hint of the preequilibrium reaction mechanism to be described later in detail in this chapter.

II.1.1 Direct Reactions

The direct reaction is a one-shot process which occurs with typical reaction time of the order of natural nuclear time ($\sim 10^{-22}$ sec). At high energies /1/ the wavelength of the incident particle in nuclear matter is so short compared to nuclear dimension that the projectile must be expected to explore the individual constituents of the target nucleus. In this approximation the trajectory of the incident particle can be considered as classical and it will only effect the nuclear matter in the immediate neighbourhood of the trajectory during the reaction time. Thus, these reactions involve the excitation of only a few of the numerous degrees of freedom available in the nucleus. Even at comparatively lower energies /2/ sometimes only a few degrees of freedom is excited., if the interaction is confined to the surface of the target nucleus and caused only a perturbation. Theoretically, therefore direct reactions are treated by Born approximation at lower energies and by impulse approximation at high energies. Since the incident particle does not interact with the nucleus as a whole but only with a small part of it, the emitted particle will take an essential part of the momentum of the incident particle giving rise to typical angular distributions. Further, the nearly negligible time difference between incidence and emission processes will lead to the occurrence of strong coherence and interference effects /2/. Consequently, the theoretical description of direct reactions involves complex coupled channel calculations.

II.1.2. Compound Nuclear Reactions:

The initial impetus to the compound nucleus theory of nuclear reactions, came from the observation of narrow resonance widths in slow-neutron absorption experiments. In 1936, Bohr /3/ explained that, the incident particle together with the target nucleus forms a compound system in which the excitation energy is first

shared among all the particles; finally after the lapse of a very long time ($\sim 10^{-15}$ sec), any one particle may gain sufficient energy to escape from the nucleus. As the life time of the compound nucleus is sufficiently long in comparison to the natural nuclear time ($\sim 10^{-22}$ sec), it is assumed that the mode of decay of the compound nucleus is independent of the mode of its formation. Thus one has to determine the cross sections of the two processes, i.e. the formation as well as the decay of the compound nucleus, in order to calculate the cross section of a compound nuclear reaction.

The decay process can be treated statistically, because of the fact that, in the energy region, where the compound nuclear reaction is valid, a large number of states may be excited, as the average level spacing in the compound nucleus is small, compared to level width. Thus when a particle gains sufficient energy, it may be emitted from any one of these levels, which can be explained only by a statistical process, as the number of excited levels is too great to be treated individually.

A quantitative description of the statistical process was first formulated by Weisskopf /4/, which was later analysed and reviewed by Bethe /5/, Blatt and Weisskopf / 6/ and Ericson /7/. A comprehensive view of the statistical theory will be presented below.

II.1.3. Statistical Model for Compound Nuclear Reaction:

In statistical process, it is assumed that a large number of states of the compound nucleus is excited through the interaction of the projectile and the nucleons of the target nucleus. Subsequent decay of the compound nucleus by particle emission, puts the system into thermal equilibrium. This happens only when a sufficient time (10^{-15} sec) has elapsed and by chance, sufficient excitation energy

has been concentrated on the particle to be emitted. It is also noteworthy that no memory of the details of the formation process is retained, except for demands of the conservation laws.

Weisskopf /4/ and Weisskopf and Ewing /8/ have carried out the first calculations on the basis of statistical model. They made use of the principle of detailed balance to calculate the probability per unit time for the compound nucleus at excitation energy E , to emit a particle ν with kinetic energy ϵ , so that the residual nuclei is left with an excitation energy U , given by

$$U = E - \epsilon - B_\nu \quad (1)$$

where B_ν is the binding energy of the particle ν in the compound nucleus.

According to the above said principle , one has

$$\left| M_{fi} \right|^2 = \left| M_{if} \right|^2 \quad (2)$$

where M_{fi} is the matrix element for the transition from the state i to the state f and M_{if} is that for the reverse process. The transition probability W_{fi} per unit time is given by

$$W_{fi} = \frac{2\pi}{\hbar} \rho_f \left| M_{fi} \right|^2 \quad (3a)$$

$$= \sigma_{fi} V_i \quad (3b)$$

where ρ_f is the density of final states per unit energy interval , σ_{fi} is the cross section for the process and V_i is the incident flux. Combing eqn.(2) and eqn.(3) one get

$$\frac{W_{fi}}{\rho_f} = \frac{W_{if}}{\rho_i} = \frac{\sigma_{if} V_f}{\rho_i} \quad (4)$$

where σ_{if} is the inverse cross section , V_f is the velocity of the emitted particle and ρ_i is the density of initial states. Eqn.(4) can be written as

$$\frac{W_{\nu}(\varepsilon, E)}{\rho_{\nu}(U)} = \frac{W(\varepsilon, U)}{\rho_c(E)} = \frac{\sigma_{\nu}(\varepsilon, U)V_{\nu}}{\rho_c(E)} \quad (5)$$

The density of states $\rho_{\nu}(U)$ is the product of the density of states of the residual nucleus per unit energy and the number of states in the momentum range dp into which the particle ν , taken to be free. The latter factor is given by

$$(2S_{\nu}+1) \frac{4\pi P^2 dp}{h^3}$$

where S_{ν} is the spin of particle ν and h is Planck's constant. Therefore the resulting transition probability is given by

$$W_{\nu}(\varepsilon, E)d\varepsilon = \frac{(2S_{\nu}+1)m_{\nu}\rho_{\nu}(U)}{\pi^2 \hbar^3 \rho_c(E)} \varepsilon \sigma_{\nu}(\varepsilon, U)d\varepsilon \quad (6)$$

where $\sigma_{\nu}(\varepsilon, U)$ is the inverse cross section for the formation of the compound nucleus when particle ν is incident upon the residual nucleus at excitation energy U and m_{ν} is the mass of particle ν and $\varepsilon = P^2 / 2m_{\nu}$. The total decay rate W_C of the compound nucleus is given by

$$W_C = \sum_{\mu} \int_0^{\infty} W_{\mu}(\varepsilon, E)d\varepsilon \quad (7)$$

where the summation is over all possible particles emitted with all possible energies

The differential cross section for the emission of the particle ν with an energy ε , which gives the energy distribution among the particle ν is

$$\frac{d\sigma_{\nu}}{d\varepsilon} = \frac{\sigma_c W_{\nu}(\varepsilon, E)}{W_c}$$

$$= \frac{\sigma_c(2S_v + 1)m_v \varepsilon \sigma_v(\varepsilon, U) \rho_v(U)}{\sum_{\mu} (2S_{\mu} + 1)m_{\mu} \int_0^{\infty} \varepsilon_{\mu} \sigma_{\mu}(\varepsilon_{\mu}, U) \rho_c(E) d\varepsilon} \quad (8)$$

Eqn.(8) takes the competition of all modes of decay into account and is known as Weisskopf Ewing evaporation formula.

Shape of the Particle Spectrum :

The shape of the particle spectrum is easily obtained. Defining entropies $S_v(U)$ and $S_c(E)$ by

$$S_v(U) = \ln \rho_v(U)$$

$$S_c(E) = \ln \rho_c(E) \quad (9)$$

$$\text{Then from eqn.(6) } W_v(\varepsilon, E) \propto e^{S_v(E-\varepsilon-B_v)-S_c(E)} \sigma_v(\varepsilon, U) \quad (10)$$

Since it is assuming that E is much greater than both the binding energy B and kinetic energy ε of the emitted particle ($E \gg B_v$, $E \gg \varepsilon$) and that S_v and S_c are identical functions ($S_v(E) = S_c(E)$). It is possible to develop

$$S_v(E-\varepsilon-B_v) = S_c(E) - (B_v+\varepsilon) \left[\frac{dS_c}{dE} \right]_E \quad (11)$$

Defining temperature $T_c(E)$ of the compound nucleus by

$$\frac{1}{T_c} = \left[\frac{dS_c}{dE} \right]$$

Eqn. (10) becomes

$$W_v(\varepsilon, E) \propto e^{-B_v/T_c(E)} \varepsilon e^{-\varepsilon/T_c(E)} \sigma_v(\varepsilon, U) \quad (12)$$

Assuming σ_p to be constant, it can be seen from the above equation, that the energy distribution of the emitted particles is Maxwellian in shape.

Inverse Reaction Cross section :

Knowledge of the inverse cross section is needed to calculate the rate, from eqn.(6). The inverse cross section is the cross section for the capture of the emitted particle by the residual nucleus in its excited state. As this is difficult to calculate or measure experimentally, one makes the usual assumption that the capture cross section for a nucleus in its excited state is equal to that in the ground state and proceeds with the calculation of these quantities from a theoretical view point. As the effects of nuclear excitation on the inverse cross sections are totally ignored, such estimates are the subject to the following uncertainties.

(I) As pointed by Ericson /7/ an excited target nucleus is expected to be less transparent to incident particles than the ground state nucleus because of fewer transitions being inhibited by the exclusion principle.

(II) The nuclear radius and diffuseness for the Wood-Saxon potential changes with increasing excitation energy, lowering the barrier for particle emission.

(III) The angular momentum may be higher for the emitting compound nucleus at high excitation than for the nucleus formed in the inverse reaction. This would result in an underestimation of the possible contribution of the higher angular momentum states to the evaporation yield.

Nuclear Level Density :

In a compound nucleus system, the loss of memory of its mode of formation leads to a decay which entirely governed by the available phase space. A dominating part in the phase space, in a nuclear reaction is played by the density of levels in the

residual nucleus. The outstanding experimental features of nuclear level density are its extremely rapid increase with excitation energy and dependence on nuclear shell and pairing effects. The rapid increase of the number of levels with excitation energy is a general characteristic of any system with a large number of degrees of freedom. In the case of simple Fermi-gas model it is assumed that the spacing of the Fermi-levels for neutrons and protons is the same and the nucleus is considered as a Fermi-gas of neutrons and protons of both spins confined to move in a sphere. This leads to level density expression /7/

$$\rho(U) = \frac{1}{12} \left(\frac{\pi^2}{a} \right)^{\frac{1}{4}} U^{\frac{-5}{4}} e^{2\sqrt{aU}} \quad (13)$$

The level density $\rho(U)$ describes the density of levels at given excitation energy U , summed over all values of angular momentum of the excited nucleus. The level density parameter 'a' is given by

$$a = 2 \left(\frac{\pi}{3} \right)^{\frac{4}{3}} \frac{m R_0^2}{\hbar^2} A \quad (14)$$

where m is the mass of a nucleon, R_0 its intrinsic radius, A is the mass number of the nucleus. So far as the theoretical estimates of the total cross section of nuclear reactions are concerned, it is enough if a simple form of the energy dependence level density is assumed, i.e.

$$\rho(U) \propto \exp \sqrt[2]{aU} \quad (15)$$

where $a = U / T^2$, T being the nuclear temperature.

A refinement of the Fermi-gas model is often made by incorporating some of the residual interactions, such as due to pairing, shell structure etc. into the level density expression by suitable modification.

Pairing Effects :

Studies on the level spacing for neighbouring nuclei have shown that the nuclear level density of a particular excitation energy depends on whether the number of neutrons or protons is odd or even. In general, it is observed that for odd A nuclei level densities are less than those for odd-odd nuclei and greater than those for even-even nuclei. This behaviour is due to the pairing energy produced by the residual part of the nucleon-nucleon force. If the amount of energy required to break one pair and cause an even-even nucleus is 2δ , then the level densities for non-even nuclei can be related to even nuclei by calculating the level densities from fictitious ground state

i.e.,

$$\rho_{\text{odd-odd}}(U) = \rho_{\text{even}}(U+2\delta)$$

$$\rho_{\text{odd}}(U) = \rho_{\text{even}}(U+\delta) \quad (16)$$

For odd-even effects seem, mainly to cause a shift of the effective excitation energy between the odd and even nuclei. The magnitude of this shift is close to the value of the pairing energy as determined from nuclear binding energies in this region.

Shell Structure Effects :

A comparison of the level spacings observed by neutron resonance in various nuclei at the same excitation energy has revealed that the level density is strongly influenced by nuclear shell structure. The density of resonances for magic or near magic nuclei is found to be one to three orders of magnitude smaller than that for nuclei between the shells upto high excitation energies. More detailed studies /9,10/ have indicated that this effect is entirely different from the odd-even effect and is closely related to the larger low energy single particle spacing in the magic nuclei rather than to shift of the entire energy scale of the excited nucleus. It might be

expected that the influence of shell effect will disappear slowly with increasing excitation energy. However, it is not known to what energies this effect will still play an important role. It is clear from a comparison of neutron resonance data with the free Fermi-gas model level density expression that such a simple theory is an inadequate explanation of nuclear level densities at moderate excitation energies.

Newton /10/ used the simple results of the equidistant spacing model but instead of using the free Fermi-gas model single particle level density value at the Fermi-level, he suggested the use of an average density of nucleon orbits in the shell model. The level density parameter 'a' is then given by

$$a = \text{const. } A^{2/3} (j_N + j_Z + 1) \quad (17)$$

where j_N and j_Z are the spin of the neutron and proton shell model states which correspond to the particular $A=N+Z$.

Another method proposed by Gilbert and Cameron /11/, while being mainly semi-empirical is very simple and has been widely used in nuclear data calculations. In the free Fermi-gas model one would expect that the ratio a/A is a constant as evident from eqn.(14). Since appreciable deviations from the expected constancy occur near closed shell nuclei, it is reasonable to try to relate shell effects in resonance spacing to the shell correction to the nuclear ground state masses. While there is no unique way of doing this, Gilbert and Cameron demonstrated that a linear relationship exists between the ratio a/A as obtained from neutron resonances and the shell correction energy S to the nuclear masses. Specifically, it was found that two linear relations

$$a/A = 0.00917 S + 0.120$$

and $a/A = 0.00917 S + 0.142$ (18)

can be obtained for the deformed and spherical nuclei respectively.

Ignatyuk et al /12 / have proposed, in addition to the shell structure effects, an energy dependence of the level density parameter a as

$$a(u)=a_{LDM} [1-f(u) S/u] \quad (19)$$

where a_{LDM} is the asymptotic value of a at high excitation energies and S is the ground state shell correction energy to the nuclear mass. The dimensionless function $f(u)$ determines the dependence of a on the excitation energy (u) as

$$f(u)=[1-e^{-\gamma u}] \quad (20)$$

The asymptotic value a_{LDM} is expressed as

$$a_{LDM}/A=\alpha+\beta A^{-1/3} \quad (21)$$

By a least square fit to the experimental level density parameters of about 200 nuclei , the following values for the coefficients were obtained $\alpha=0.114$, $\beta=0.162$, $\gamma= 0.054 \text{ MeV}^{-1}$.

Another semiempirical formula for level density was proposed by S.K.Kataria et al /13/ which takes into account the influence of nuclear shell structure on level densities and the excitation energy dependence of shell effects. The formulation is based on the results of investigation of the thermodynamic properties of nuclei and has a built-in excitation energy dependence of shell effects on the level densities. The formula involves mass-independent parameter characterising the average single particle level density near the Fermi level and the wavelength of shell oscillations. For a non-interacting Fermi-gas confined to a finite volume, the level density parameter , a can be expressed as

$$a= \gamma' A(1-\beta' A^{-1/3} B_S) \quad (22)$$

where B_S is the ratio of the area of nuclear surface to that of a sphere having the same volume ($B_S > 1$ for deformed nuclei) and γ' , β' are mass-independent constants. The best values of γ' and β' , obtained by a least-square fit to the experimental data, are $\gamma' = 0.176 \text{ MeV}^{-1}$ and $\beta'=1.0$.

II.2 Theory of Preequilibrium Models :

As the isochronous cyclotron came into wide usage in the 1960's and higher projectile energies become available, the compound nucleus mechanism recedes to the background, giving place to preequilibrium phenomena. As already pointed out, precompound reactions occupy a stage intermediate between the direct and compound nuclear reactions. As such the characteristics of such reactions are also midway between the characteristics exhibited by the direct and compound nuclear processes. As the composite nucleus proceeds towards statistically equilibrium the projectile energy and momentum are shared between more and more particles after each successive interaction. In the initial stages when the number of interactions is small the energy available to each degree of freedom is comparatively large. Consequently, the particles emitted at these stages will carry more energy than those emitted from the equilibrated compound nucleus. This qualitatively accounts for the high energy tail of the excitation function. Also, in the initial stages of the precompound process the composite nucleus retains the memory of the projectile direction as a result of which the emission spectrum from these initial stages is preferentially forward peaked as in the case of direct reactions. However, in the later stages, as the number of degrees of freedom increases the memory of the projectile direction gets more and more diffused and the ejectile spectrum tends towards isotropy. This means that though the precompound ejectile shows forward peaking it also exhibits substantial cross sections in the backward angles as well.

The existing models which describe this preequilibrium phase of reaction may be divided into two groups: Quantum mechanical models and Semi-classical models. The latter are not only easy to use but also transparent in their formulation. In the following sections we first discuss the models for angle integrated energy spectra and then the models for describing angular distribution.

II.2.1 Exciton Model :

To explain the new features of particle spectra, J. J. Griffin /14/ proposed a “precompound” model. The basic idea of the model is that the incident particle and the target nucleus together form an excited “ compound system” which is different from the usual compound nucleus. This system is a relatively short-lived compound state which is assumed to decay by a weak two-body residual interaction. The eigen states of the system are classified according to the number of particles and holes (commonly referred to as “excitons”) excited from the even-even ground state in an independent particle picture. The nature of the interaction causes only such energy conserving transitions in which the exciton number changes by 0 or ± 2 . Thus, for example, if the initial state in a nucleon induced reaction is characterised by $n_0=1$, then the successive two body collision of the incident particle with one of the target nucleons might change the energy of the incident particle and produce a particle-hole pair creating a system with $n_0=3$. The next collision between one of the two excited particles and a nucleon in the Fermi sea might create the following states: (i) $n_0=5$ (creation of a new particle-hole pair), (ii) $n_0=1$ (one of the particle fills the hole), (iii) $n_0=3$ (a different 2p-1h state is formed). In the binary collision if the nuclear particle is raised well above the Fermi sea into the continuum., then nucleon emission takes place. Such possibilities exist at each of the successive n-exciton states unless all the excitons have energies less than the binding energy. This phenomenon is usually referred to as “Preequilibrium emission” (of particles) or “Preequilibrium decay” (of the compound system). A schematic representation of the first few stages of the reaction in the precompound model is shown in figure II.1

The model actually describes the approach to equilibrium of the system. For small numbers of particles and holes, the process will move predominantly to increase the exciton number since the density of states (to be shown shortly) is a

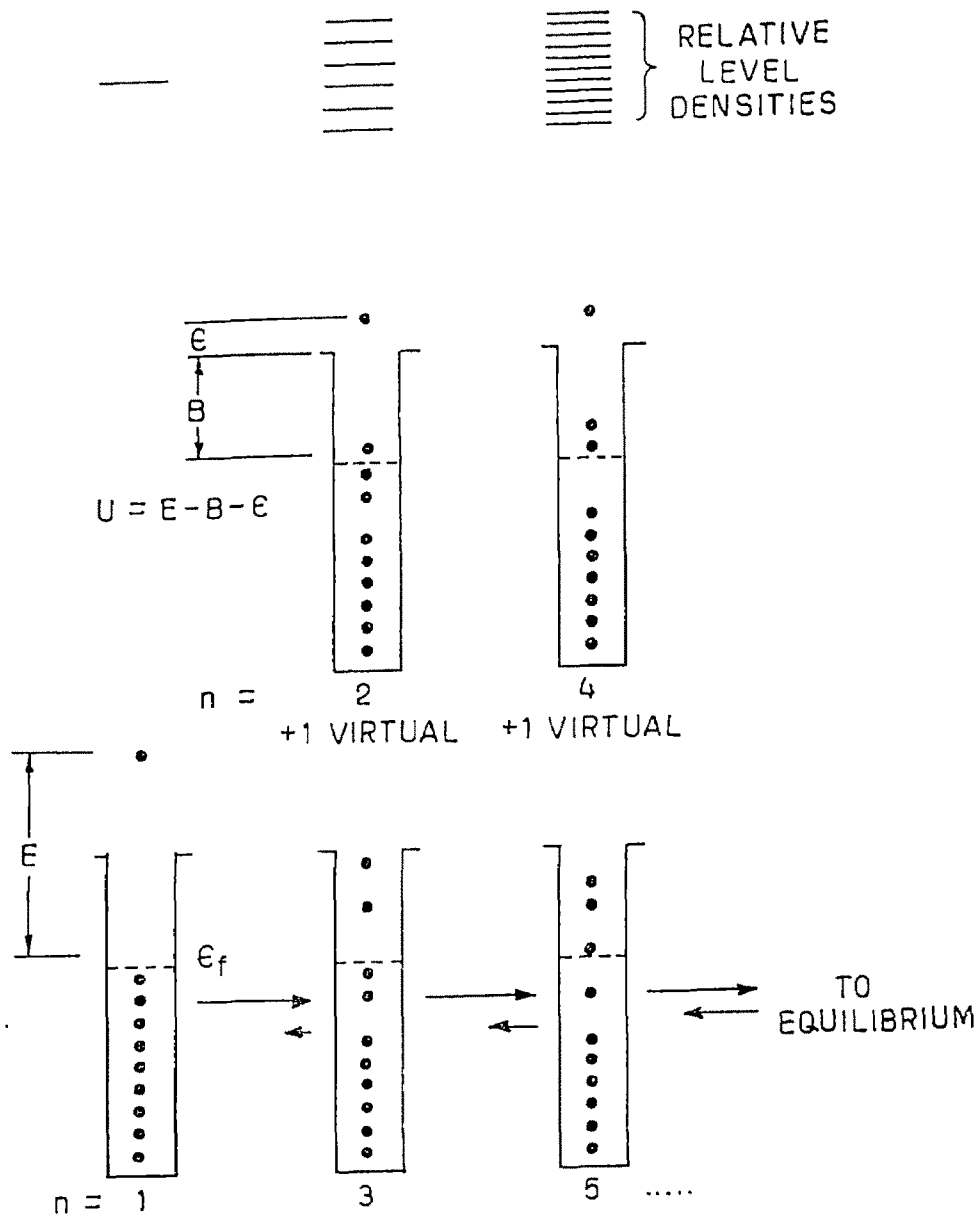


Fig.II.1 SCHEMATIC REPRESENTATION OF THE EQUILIBRATION PROCESS BY PARTICLE-HOLE EXCITATIONS IN THE EXCITON MODEL

rapidly increasing function of $p+h$. At some point, pair annihilation will tend to drive the process backward and a steady-state, or equilibrium, condition is reached.

An expression of the density of particle-hole states which are accessible to a nucleus with excitation U is given by Ericson /7/

$$\rho_{p,h}(U) = \frac{g^{p+h} U^{p+h-1}}{p! h! (p+h-1)!} \quad (23)$$

Here $g=d^{-1}$, where d is the single particle level spacing. In eqn.(23) an equidistant spacing for a Fermi gas model was used. It is seen that for a sufficient number of particles and holes the expression in the denominator increases faster than the exponential in the numerator, decreasing the density of states. The approximate number of excitons \bar{n} at equilibrium can be obtained by differentiating eqn.(23) to find a maximum, assuming $n=p+h$ and $p \approx h \approx n/2$. The result is

$$\bar{n} \approx (2gU)^{1/2} \quad (24)$$

The transition rates $\lambda_{nn'}$ from an n -exciton state to an n' -exciton state ($n'=n$ or $n \pm 2$), using the Golden Rule, is given by

$$\lambda_{nn'} = \frac{2\pi}{\hbar} |M|^2 \rho_n(U) \quad (25)$$

Lack of knowledge of the size of the square of the matrix element, $|M|^2$ makes it impossible to determine $\lambda_{nn'}$, except on a relative basis. It is at this point that the model becomes phenomenological. Also, this expression assumes that all states in a given p and h configuration are accessible, for example, from a $p-1$, $h-1$ configuration. This is not valid, as the accessible states are only those which can be reached by scattering one excited particle with a ground state particle or by rearrangement of the particles and holes by operating with two annihilation and two creation operators. Other states are accessible only by two or more scattering events. Incorporating the above, Williams /15/ obtained the following transition rates

$$\lambda_{n,n+2} = \lambda_+ = \frac{2\pi}{\hbar} |M|^2 \frac{g^3 U^2}{(p+h+1)} \quad (26a)$$

$$\lambda_{n,n-2} = \lambda_- = \frac{2\pi}{\hbar} |M|^2 g[p \cdot h \cdot (p+h-2)] \quad (26b)$$

$$\lambda_{n,n} = \lambda_0 = \frac{2\pi}{\hbar} |M|^2 g^2 U \left[\frac{3(p+h)-2}{4} \right] \quad (26c)$$

Here λ_+ , λ_- , λ_0 are the transition rates for the exciton number increasing by two, decreasing by two, and remaining the same, respectively.

At equilibrium $\lambda_+ = \lambda_-$, assuming $p \approx h \approx n/2$, leads once again to eqn.(24). The probability per unit time of emission of a particle with channel energy between ε and $\varepsilon+d\varepsilon$ from an n -exciton state is

$$W_n(\varepsilon)d\varepsilon = (2S_\nu + 1) \frac{4\pi P_\nu^2}{h^3} \sigma_\nu(\varepsilon, U) \left[\frac{\rho_{n-1}(U)}{\rho_{n(E)}} \right] d\varepsilon \quad (27a)$$

where $P_\nu^2 = 2m\varepsilon$, $\hbar = h/2\pi$ and $\sigma_\nu(\varepsilon, U)$ is the inverse cross section, for the capture of particle ν by the residual nucleus at excitation U .

The eqn.(27a) may be written as

$$W_n(\varepsilon)d\varepsilon = (2S_\nu + 1) \frac{m\varepsilon}{\pi^2 \hbar^3} \sigma_\nu(\varepsilon, U) \left[\frac{\rho_{n-1}(U)}{\rho_{n(E)}} \right] d\varepsilon \quad (27b)$$

In this form, it is completely analogous to eqn.(6) for the evaporation of a compound nucleus with only the functional form of the level densities being different. The smooth transition between preequilibrium and equilibrium emission is apparent. Of course, the preequilibrium emission given by eqn.(27) occurs only over a time span determined by τ_n is the mean life of the n -exciton state determined by the transition rates, e.g. eqn.(26).

As pointed out earlier and as seen in eqn.(26), the rate λ_+ is much greater than λ_- and λ_0 for the small initial values of $n = p = h$. So it may be safely assumed that λ_+ dominates in the initial stages when most of the higher energy non-compound particles are emitted.

Under these circumstances, the particle emission from the n^{th} exciton state is given by

$$P_n(\varepsilon) = W_n(\varepsilon) \tau_n(E) \quad (28)$$

where $\tau_n(E)$ is the mean life time of the n -exciton and depends on the total excitation energy E , but not on the individual energies of the excitons (ε).

The total probability of emission of a particle between energy ε and $\varepsilon+d\varepsilon$ is given by the contributions from all the exciton states,

$$P(\varepsilon)d\varepsilon = \sum_{\substack{n=n_0 \\ \Delta n = +2}}^{\bar{n}} F_n P_n(\varepsilon) d\varepsilon \quad (29)$$

where n_0 and \bar{n} are the initial and equilibrium values of exciton numbers.

F_n is a 'depletion factor', which gives the fraction of the initial distribution which survives to the n -exciton state without emitting a particle and is given by

$$F_n = \prod_{n'=n_0+2}^n (1 - P_{n'-2}) \quad (30)$$

where $P_{n'-2}$ is the fraction of the n -exciton population that decayed through particle emission. The eqn.(29) may be written as

$$P(\varepsilon)d\varepsilon = \sum_{\substack{n=n_0 \\ \Delta n = 2}}^{\bar{n}} F_n \left[\frac{\rho_{n-1}(U)g}{\rho_n(E)} \right] \left[\frac{\lambda_c(\varepsilon)}{\langle \lambda, (n, E) \rangle} \right] \quad (31)$$

The logic of eqn.(31) is transparent. The expression in the first square bracket is the particle state density P_d , which is fraction of the population of the n -exciton state that if emitted, would result in a particle with energy ε to $\varepsilon+d\varepsilon$ in the continuum. The second square bracket is the ratio of rate of decay into the continuum to the total transition rate for an internal transition as well as for emission into the continuum.

Here

$$\lambda_c(\varepsilon) = (2S_\nu + 1) \frac{m\varepsilon}{\pi^2 \hbar^3 g} \sigma_\nu(\varepsilon, U) \quad (32a)$$

is the rate of emission of particles which would have channel energy between ε and $\varepsilon+d\varepsilon$ in the continuum, and $\langle \lambda_+(n, E) \rangle$ is the average intranuclear transition rate of an n -exciton state. This transition is brought about by any one of the n -excitons having a binary collision with a nucleon below the Fermi sea and creating an extra particle-hole pair, and is given by

$$\langle \lambda_+(n, E) \rangle = \frac{1}{\tau_n(E)} \quad (32b)$$

Substituting for the exciton densities from eqn.(23) into eqn.(31), the total probability of emission of a particle can be written as

$$P(\varepsilon)d\varepsilon = (2S_\nu + 1) \frac{m\varepsilon}{\pi^2 \hbar^3 gE} \sigma_\nu(\varepsilon, U) \sum_{\substack{n=n_0 \\ \Delta n = 2}}^{\bar{n}} \left(\frac{U}{E} \right)^{n-2} P(n-1) \tau_n(E) d\varepsilon \quad (33)$$

For a given exciton state, some fraction of the state will have one or more particles with energy in excess of the binding energy, at least until a particle is emitted. The probability of a single particle having a sizable fraction of the incoming energy decreases quickly with increasing exciton number, since the total phase space eqn. (23) increases as $(gE)^{n-1}$. This is manifested by the $(U/E)^{n-2}$ dependence of $P(\varepsilon)$ in eqn.(33). Therefore, merely from phase space arguments, the Exciton model predicts

that emission of high energy particle occurs in the first stages of the reaction since high ϵ implies low $U(E-\epsilon -B_v)$ and $(U/E)^{n-2}$ becomes vanishingly small for large n .

II.2.2 Master Equation Model :

The corner stone of this non-equilibrium statistical model is the assumption that the incoming projectile by interacting with the target nucleus gives rise to a simple initial configuration characterized by a small number of particles above and holes below the Fermi sea which are called 'excitons'. Successive two-body residual interactions of the particle-particle and hole-hole type make up an 'intranuclear cascade' which eventually leads to the compound nucleus state through a sequence of states characterized by an increasing exciton number. At each stage of this equilibration process there is competition between two decay modes of the composite system, namely, the decay by particle emission and the decay by exciton-nucleon interaction. A schematic representation of evolution of the reacting system is shown in figure II.1 For example, if the initial state in a nucleon induced reaction is characterized by $n_0=1$, then the successive two-body collision of the incident particle with one of the target nucleons might change the energy of the incident particle and produce a particle-hole pair creating a system with $n_0=3$ (in Exciton model, all possible $n_0=3$ states are equally probable). The next collision between one of the two excited particles and a nucleon in the Fermi sea might create the following states: (i) $n_0=5$ (creation of a new particle-hole pair), (ii) $n_0=3$ (a different 2p-1h state is formed). Thus, during the equilibrating process the binary interactions may change the exciton number by +2, 0, or -2 and this is described by the master equation of Pauli /16/as

$$\frac{dP(n,t)}{dt} = P(n-2,t)\lambda_+(n-2,E) + P(n+2,t)\lambda_-(n+2,E) - P(n,t)\lambda_+(n,E) - P(n,t)\lambda_-(n,E) + L(n,E) \quad (34)$$

where $P(n,t)$ = the probability of excitation of n excitons from the Fermi sea

λ = transition probabilities for the creation (+) or destruction (-) of one particle-hole pair.

$L(n,E)$ = particle emission probability from an n exciton state,

The initial condition for the master equation is

$$P(n,t=0) = \delta n n_0$$

For nucleons the initial condition usually adopted is

$$n_0 = 3, p_0 = 2, h_0 = 1$$

Total time spent by the composite system in the n exciton state is computed as

$$T(n,E) = \int_0^{\infty} P(n,t) dt \quad (35)$$

II.2.3 Intranuclear Transition Rate :

The internal transition rates λ_+ , are calculated using either of the following semi-empirical approach or two theoretical approaches.

(a) Semi empirical Approach using Fermi's Golden Rule :

To evaluate the transition probabilities we need to know λ_+ , λ_- and λ_0 . They are often discussed in a form which was first derived by Williams /15/ from the Golden rule for transition probabilities as given by eqn.(26). Here $|M|^2$ is the average squared matrix element of the transitions. $|M|^2$ is frequently treated simply as a fit parameter. In this case only relative spectral shapes rather than absolute cross section can be calculated. A more elaborate prescription for the determination of

$|M|^2$ is due to Braga-Marcazzan et al /17/ who used the Fermi gas model. As a result of this analysis Kalbach-Cline /18/ has proposed the following mass number and energy dependence

$$|M|^2 = KA^{-3}E^{-1} \text{ MeV}^2, K = 190(\pm 32\%)\text{MeV}^3 \quad (36)$$

As can be seen $|M|^2$ is independent of the exciton number. A later empirical expression /18a/ includes a dependence on n :

$$\begin{aligned} |M|^2 &= KA^{-3}e^{-1}(e/7\text{MeV})^{1/2} (e/2\text{MeV})^{1/2} \quad \text{for } e < 2\text{MeV} \\ &= KA^{-3}e^{-1}(e/7\text{MeV})^{1/2} \quad \text{for } 2\text{MeV} \leq e \leq 7\text{MeV} \\ &= KA^{-3}e^{-1} \quad \text{for } 7\text{MeV} \leq e \leq 15\text{MeV} \\ &= KA^{-3}e^{-1}(15\text{MeV}/e)^{1/2} \quad \text{for } e > 15\text{MeV} \end{aligned} \quad (37)$$

where $e = E/n$ and $K = 135 \text{ MeV}^3$

(b) Intranuclear Transition Rates from Nuclear Matter Approach :

Braga-Marcazzan et al /17/ attempted to remove all adjustable parameters and thus to obtain absolute cross section. They equated the internal transition rate λ_{\pm} , with the nucleon-nucleon collision rate in an infinite nuclear matter as

$$\lambda_{\pm} = \rho V \langle \sigma \rangle \quad (38)$$

where ρ is the density of nucleons and V is the velocity of particle in nuclear matter given by

$$V = [2(E+E_F) / m]^{1/2} \quad (39)$$

$\langle \sigma \rangle$ is the effective cross section for an excited nucleon to interact with the other nucleons for which a Fermi gas momentum distribution is assumed. The average indicated by $\langle \rangle$ is taken over the free nucleon-nucleon scattering cross section with a method due to Goldberger /19/ and Kikuchi and Kawai /20/ with Pauli principle taken into account. On this basis Gadioli et al /21/ calculated λ_{\pm} for a truncated harmonic oscillator potential and for a square well, taking into account the finite

potential depth not only for the exciton transition probabilities but also for the exciton state densities. For the harmonic oscillator well with 40 MeV Fermi energy at the centre they found results which were only slightly different from those of square well with 20 MeV Fermi energy. For the later case their results show a quadratic increase of λ_+ upto an excitation energy of 10MeV and a linear increase for higher energies. This means that $|M|^2$ is independent of excitation below 10 MeV whereas above 10 MeV the energy dependence of Kalbach-Cline /18/ is valid. Gadioli et al /21/ were able to reproduce absolute differential cross section of (p,n) reactions as well as their excitation functions for a wide range of mass numbers ($89 \leq A \leq 169$) and excitation energies ($15 \text{ MeV} \leq E \leq 50 \text{ MeV}$) provided they reduced their λ_+ values generally by a factor of 4 ± 1 .

(c) Intranuclear Transition Rates from the Imaginary Optical Potential :

The use of the optical potential in calculating intranuclear transition rates for pre equilibrium decay models offers distinct advantages. The parameters of the optical potential have been determined from a large body of experimental data. The mean free path values are therefore based on experimental measurements in nuclear matter, as opposed to the extrapolation of free nucleon-nucleon scattering cross sections to nuclear environment. Becchetti and Greenless /22/ have analysed a large body of data to find a “best set” of optical parameters for nucleon induced reactions. The mean free path is related to the absorptive (imaginary) part of the optical potential. A complex wave number can be defined as

$$K = [2m / \hbar^2 (E + E_F + iV_1)]^{1/2} \quad (40)$$

$$= K_r + iK_i$$

If $V_1 \ll E_F + E$, then

$$K_r = \left[\frac{2m(E + E_F)}{\hbar^2} \right]^{1/2} \quad (41)$$

$$K_i = \frac{1}{2} \left[\frac{V_I}{E + E_F} \right] K_r \quad (42)$$

The wave function is then

$$\psi = e^{iK_r x} e^{-iK_i x}$$

the 'decay length' of $\psi\psi^* = e^{-2K_i x}$ determines the mean path.

$$MFP(E) = \frac{1}{2K_i} = \frac{E + E_F}{V_I K_r} = \frac{\hbar V}{2V_I} \quad (43)$$

where V is the velocity of the nucleon of kinetic energy (E+E_F) and transition rate is simply given by

$$\lambda_+(\varepsilon) = \frac{V}{MFP(E + E_F)} = \frac{2V_I}{\hbar} \quad (44)$$

The values of internal transition rate obtained by this method agree very well with those derived through nuclear matter approach.

II.2.4 Fermi Gas Equilibrium Model :

Both the Exciton model and the Master Equation model assume that all energy partitions between particles and holes in a given exciton state occur with equal a priori probability. However, the energy distribution of the excited degrees of freedom (excited particles and holes) may play a significant role in determining the precompund energy spectrum. This aspect of the preequilibrium phenomenon was first studied by Harp, Miller and Berne/23,24/ independently of the Exciton model approach. The Harp-Miller-Berne (HMB) model is shown schematically in figure II.2 . The nuclear single particle states are classified according to their energies in groups or "bins" whose size $\Delta\varepsilon$ is chosen to be of some convenient

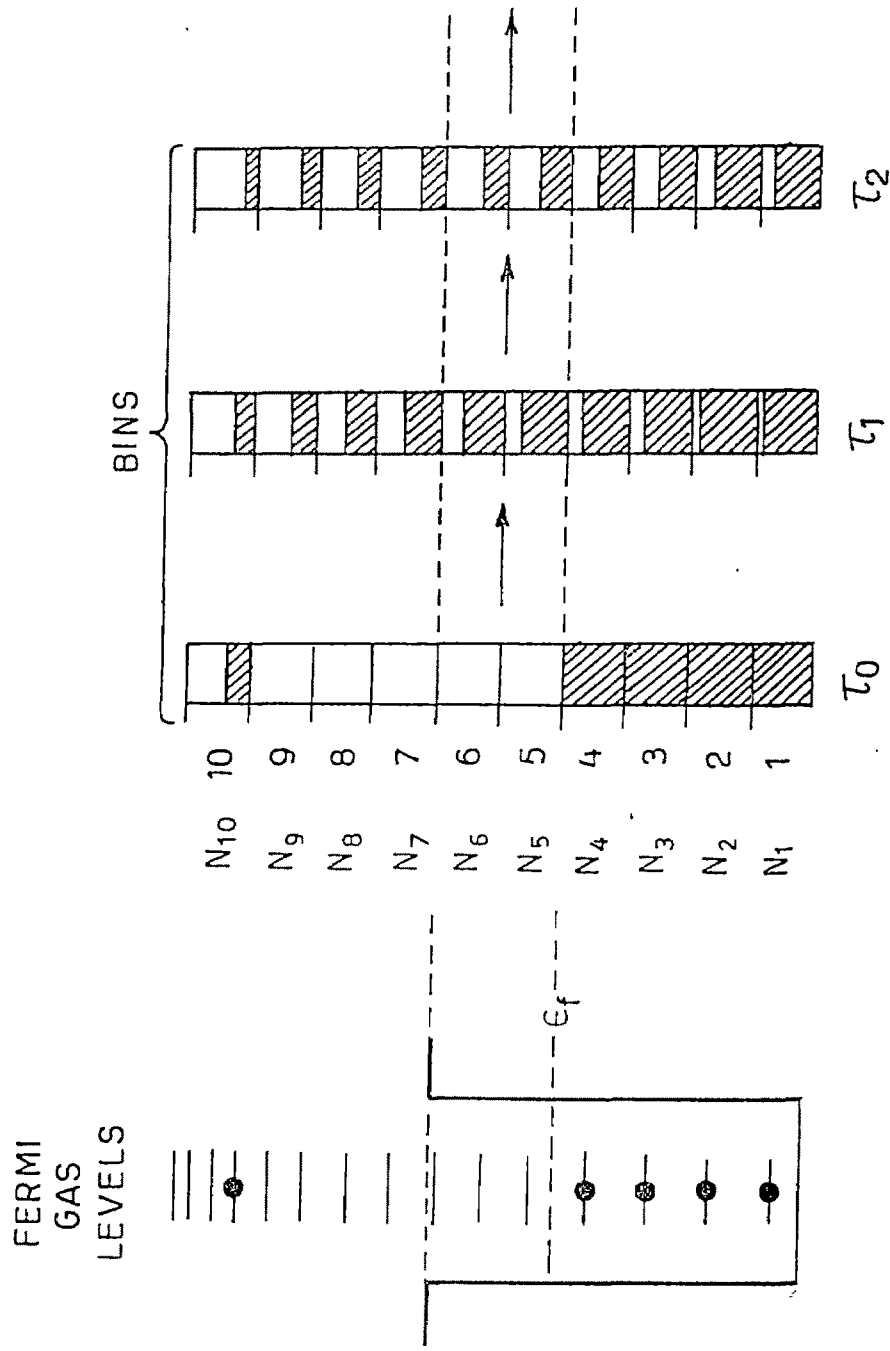


Fig.II.2 SCHEMATIC REPRESENTATION OF THE EQUILIBRATION PROCESS IN THE HARP-MILLER-BERNE MODEL

dimension. The model calculates the occupation probability of an average state in the i^{th} bin as a function of time. At the start of the reaction all levels below the Fermi energy are filled up (since the target is in its ground state) and the projectile is in an excited state. This gives the bin occupation probabilities at time $\tau=\tau_0$. Two body interactions then lead to a redistribution of probabilities. This goes on until a steady state configuration is reached. At each time during the equilibration process the energy spectrum of emitted nucleons are calculated and a net spectrum obtained.

The basic assumptions of the model are (1) interactions within the nucleons arise from nucleon-nucleon scattering and thus two nucleons are always involved going from two initial states to two final states; (2) the transition probabilities are dependent only on the energies of the particles involved in the scattering (and not also on the final state densities as in the Exciton model); (3) the transition probabilities vary slowly with energy over some interval $\Delta\varepsilon$ so that a constant value of the transition probability may be used for all levels within a bin of energy interval $\Delta\varepsilon$.

There are several interesting features of the HMB model. The first is that it gives the time evolution of the equilibration process (this is also true of the Master Equation model). The second is that it calculates the transition rates from nucleon-nucleon scattering cross sections and thus avoids the uncertainties involved in the calculation of $|M|^2$ of the Exciton model or the Master Equation model. The third feature is that so far the free Fermi gas model has been used to determine the bin occupancy but it is possible to use more realistic models like Nilsson orbitals to investigate nuclear structure effects.

III.2.5 Hybrid Model :

The Hybrid model was developed by Blann /25,26/ and is a “marriage” between Griffin Exciton model and the Fermi gas equilibrium model of Harp, Miller and Berne.

The similarities to the Griffin Exciton model are on the following points:

(i) Equally spaced single particle levels are used. The $\varepsilon^{1/2}$ dependence of the HMB model is more realistic but does not lend it itself to a simple expression of the exciton level density as in eqn.(23) and therefore it is not used;

(ii) Equal population probabilities based on the intermediate state level densities eqn.(24) are assumed ;

(iii) A closed form approach as in eqn.(33) has been used instead of a more rigorous master equation solution as in eqn.(34). The former approach is computationally simpler but is not quite valid as the equilibrium is reached.

Similarities to the Fermi gas equilibrium model:

Transition rates λ_+ of the excited particles were determined as in the HMB model, from calculation of the mean free paths of nucleons in nucleon-nucleon scattering (Pauli corrected) or from the imaginary potential of the optical model.

As in Exciton model the total particle emission probability, $P(\varepsilon)d\varepsilon$, in a given channel energy range, ε and $\varepsilon+d\varepsilon$, is given as a sum over the contributions of the intermediate states , although here this has significance as a statistical book-keeping

operation rather than an absolute time basis. The sum is taken from some initial number of excitons n_0 to the equilibrium number \bar{n} , in the same way as in the Exciton model (see eqn.(31)). The emission probability in the Hybrid model is given by

$$P(\varepsilon)d\varepsilon = \sum_{\substack{n=n_0 \\ \Delta n = 2}}^{\bar{n}} F_n \left[\frac{\rho_{n-1}(U)g}{\rho_n(E)} \right] \left[\frac{\lambda_c(\varepsilon)}{\lambda_+(\varepsilon) + \lambda_c(\varepsilon)} \right] \quad (45)$$

Where F_n and $\lambda_c(\varepsilon)$ are defined as in eqn.(30) and eqn.(32a) respectively. $\lambda_+(\varepsilon)$ is the intranuclear transition rate corresponding to a particle of energy ε , which means the probability for the creation of a particle-hole pair in binary collision between the excited particle and a nucleon below the Fermi sea.

The logic of eqn.(45) is transparent. The expression in the first square bracket is the particle state density P_d , which is the fraction of the population of the n -exciton state that if emitted, would result in a particle with energy ε to $\varepsilon + d\varepsilon$ in the continuum to the total transition rate for an internal transition as well as for emission into the continuum.

This expression demonstrates the single particle energy (ε) dependence of the transition rate in contrast to the rate used in the Exciton model eqn.(31) which depends on the total excitation energy E .

The rate of particle emission will be different for protons and neutrons due to Coulomb effects. To take this effect into account eqn.(45) may be modified as

$$P(\varepsilon)d\varepsilon = \sum_{\substack{n=n_0 \\ \Delta n = 2}}^{\bar{n}} F_n \left[{}_n f_v \frac{\rho_{n-1}(U)g_v}{\rho_n(E)} \right] \left[\frac{\lambda_c(\varepsilon)}{\lambda_+(\varepsilon) + \lambda_c(\varepsilon)} \right]$$

$$= \sum_{\substack{n=n_0 \\ \Delta n = 2}}^{\bar{n}} {}_n P_v(\varepsilon) d\varepsilon \quad (46)$$

where v denotes neutron or proton, ${}_n f_v$ is fraction of particle of types v in an n -exciton state and ${}_n P_v(\varepsilon)$ is probability of emitting nucleon of type v with channel energy ε , from an n -exciton state.

In practise, ${}_n f_v$ is determined as follows : Initially a certain ratio of protons and neutrons is assumed among the particles of the initial stage and these numbers are increased by 0.5 for each succeeding value of n . Typical initial values for neutrons and protons for proton induced reaction calculation are 0.8 and 1.2 respectively, with $n_0 = 3$ (corresponding to a 2p-1h state as initial state). An alpha induced reaction might use 2.0 for both neutrons and protons with $n_0 = 4$ (corresponding to 4p0h initial state).

Level densities $\rho_{n-1}(U)$ and $\rho_n(E)$ as obtained from eqn.(24), allow configurations which violate Pauli exclusion principle. A simple correction is provided /15/

$$\rho_n(U) = \frac{g(gU - A)^{n-1}}{p!h!(n-1)!} \quad (47a)$$

$$\text{where } A = 1/4 (p^2 + h^2) + 1/4 (p - h) - 1/2 h \quad (47b)$$

The transition rate $\lambda_+(\varepsilon)$ from nucleon-nucleon scattering can be obtained from

$$\lambda_+(\varepsilon) = \frac{V}{MFP(E)} \quad (48)$$

where V is the velocity of a nucleon of energy $E (= \varepsilon + E_F + B)$, where E_F is the Fermi energy and B is the binding energy) and $MFP(E)$ is the mean free path. First, the free nucleon-nucleon cross section are calculated from empirical relationships with $\beta = V/C$ /20/.

$$\sigma_{PP}(E) = \sigma_{NN}(E) = \left(\frac{10.63}{\beta^2} - \frac{29.92}{\beta} + 42.9 \right) \text{mb} \quad (49)$$

$$\sigma_{NP}(E) = \left(\frac{34.10}{\beta^2} - \frac{82.2}{\beta} + 82.2 \right) \text{mb} \quad (50)$$

The effective cross section, $\bar{\sigma}(E)$ are corrected for the effects of the pauli principle by /20/.

$$\bar{\sigma}(E) = \sigma(E) P(E_F / E) \quad (51)$$

where $\sigma(E)$ is the free nucleon - nucleon scattering cross section and $P(E_F / E)$ is the function

$$P(E_F / E) = 1 - 7/5 X, \quad X \leq 1/2 \quad (52a)$$

$$P(E_F / E) = 1 - 7/5 X + 2/5 X (2 - X^1)^{5/2}, \quad X \geq 1/2 \quad (52b)$$

The average effective cross section $\langle \bar{\sigma}(E) \rangle$, for a nucleon of type ν at energy E within a nucleus of A nucleons and Z protons is then

$$\langle \bar{\sigma}(E) \rangle_{\nu} = [(A - Z) \bar{\sigma}_{NX}(E) + Z \bar{\sigma}_{PX}(E)] / A \quad (53)$$

The mean free path is given by

$$MFP(E) = \frac{1}{\rho \langle \bar{\sigma}(E) \rangle_{\nu}} \quad (54)$$

where ρ is the nuclear matter density and is defined as number of nucleons per unit nuclear volume

$$\rho = \frac{A}{\frac{4}{3} \pi R^3} \quad (55)$$

Where R is nuclear radius and is equal to $R_0 A^{1/3}$; R_0 = single nucleon radius.

$$\rho = \frac{A}{\frac{4}{3} \pi R_0^3 A} = \frac{3}{4 \pi R_0^3} \quad (56)$$

Substituting eqn.(54) into eqn.(48) yields

$$\lambda_+(\varepsilon) = V\rho \langle \bar{\sigma}(E) \rangle_v = \rho \langle \bar{\sigma}(E) \rangle_v \sqrt{\frac{2(\varepsilon + E_F + B)}{m}} \quad (57)$$

Mean free paths from the optical model may also be used to evaluate $\lambda_+(\varepsilon)$ as discussed in section 2.3(c).

II.2.6 Geometry Dependent Hybrid Model :

Each of the phase space models discussed so far have one important defects in that they do not explicitly consider the geometry of the nucleus. This has been rectified by Blann /27/. He has taken the effects of interaction in the diffuse nuclear surface as the equilibration process proceeds, i.e. the importance of longer mean free paths in the diffuse edge of the nucleus where the density is small. He divided the nucleus into zones, the population of each zone being determined by the transmission coefficient T_l for the partial populating zone. The particle emission is then calculated as a sum over all the zones.

$$\sigma_v(\varepsilon) d\varepsilon = \pi \lambda^2 \sum_{l=0}^{\infty} (2l+1) T_l P_v(\varepsilon) d\varepsilon \quad (58)$$

where $\pi \lambda^2 (2l+1) T_l$ is the reaction cross section of the l^{th} partial wave and T_l is the transmission coefficient .

According to the Thomas-Fermi model the Fermi energy decreases with the nuclear density, $\rho(r)$, towards the surface as

$$E_F(r) = \frac{\hbar^2}{2m} \left[\frac{3}{2} \pi^2 \rho(r) \right]^{2/3} \quad (59)$$

where $\rho(r)$ follows the Wood-Saxon distribution given by

$$\rho(r) = \rho_s \left[\exp \frac{r-c}{z} + 1 \right]^{-1} \quad (60)$$

where c is the nuclear half-density radius equal to $1.07A^{1/3}$ fm , z is the surface thickness equal to 0.55 fm and $\bar{\rho}_s$ is the saturation density at the centre equal to $[4/3\pi 1_0^3]^{-1}$.

The surface diffuseness effect can be obtained by averaging the nuclear density along the particle trajectory with the impact parameter $R_l = (1+1/2) \lambda$ as the lower limit and $R_s = c+5z$ as the upper limit. The average density is then given by

$$\bar{\rho}(R_l) = \left[\frac{1}{(R_s - R_l)} \right] \int_{R_l}^{R_s} \rho(r) dr \quad (61)$$

Thus, the Fermi energy is obtained as

$$E_F(R_l) = E_F \left[\bar{\rho}(R_l) / \rho_s \right]^{2/3}$$

$$\text{where } E_F = \frac{\hbar^2}{2m} \left[\frac{3}{2} \pi^2 \rho_s \right]^{2/3} \text{ is the usual Fermi energy.} \quad (62)$$

For the correct evaluation of transmission coefficient Blann and Vonach/28/ have modified the parameter c as

$$c = 1.18A^{1/3} \left[1 - \frac{1}{(1.18A^{1/3})^2} \right] + \lambda \quad (63)$$

where λ is an adhoc range parameter, the single particle level density, g_b in the above eqns. for neutrons is given by

$$g_n = N/20 [(E_F + B_n + \epsilon_n) / E_F]^{1/2} \quad (64a)$$

$$g_p = Z/20 [(E_F + B_p + \epsilon_p) / E_F]^{1/2} \quad (64b)$$

using the above relation Blann has computed

$$\rho_{1plh} = g E_F(R_l) \quad \text{for } U > E_F(R_l) \quad (65a)$$

$$\rho_{2plh} = 1/4 g^2 E_F(R_l) 2E - E_F(R_l), \text{ for } E > E_F(R_l) \quad (65b)$$

In all other cases the Williams formula is used to calculate the state level densities.

λ_{coll} is now given as

$$\lambda_{\text{coll}}^1(\epsilon) = 2V_I(R_1)/\hbar \quad (66)$$

$$\text{with } V_I(R_1) = \frac{1}{R_s - R_l} \int_{R_l}^{R_s} V_I(r) dr \quad (67)$$

$$\text{and } V_I(r) = -\frac{V_I}{1 + e^{(R_0 - r)/a}} \quad (68)$$

where V_I is the corresponding imaginary term of the optical potential and $R_s = R_0 A^{1/3} + 5a$, where $R_0 = 1.32$ fm and $a = 0.51 + 0.7(N-Z)/A$ fm.

It may be remarked that both the Hybrid and Geometry Dependent Hybrid models therefore give only the preequilibrium contribution and to obtain the equilibrium component Weisskopf-Ewing evaporation model is employed.

It may be pointed out that there are some salient difference between the physical concepts of Hybrid model and Exciton model. In the Hybrid model the transition rate refers to an individual particle whereas in the Exciton model it refers to the average decay rate of the states of given exciton configuration. There has been a prolonged controversy /29,29a/ that was resolved by Ernst and Rama Rao /30/ and by Bisplinghoff /31/.

II.2.7 Preequilibrium Models for Complex Particle Emission :

Preequilibrium emission of complex particles is treated only in the framework of Exciton model, on the basic assumption of pre formation of clusters or by introducing a term representing the probability of cluster formation at the time of emission. The first assumption receives partial justification from the possibility of existence of clusters in the nuclear surface region, where the density is low and Pauli exclusion principle may not be valid. The second idea seems to be inspire by the possibility of strongly “correlated motion” among some of the emitted nucleons. The

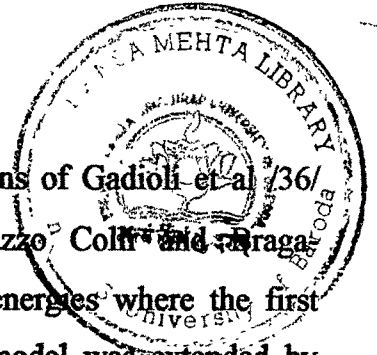
earlier models on the study of complex particle emission have been restricted to α -particles only.

(a) Model of Preformed α -particles :

This model was proposed by Millazzo Coili and Braga-Marcazzan /32/ while analysing the spectra from (n,α) reaction on nuclei with $A \geq 130$.

The basic assumption of the model is that α -particle is preformed in the target nucleus in its ground state. This preformed α -particle gets excited during the projectile-target interaction and eventually be emitted from the composite system. It is assumed that the excited α -cluster behaves as a single exciton. The cluster is visualised as a group of four strongly correlated target nucleons with $\epsilon_\alpha = \epsilon/4$ single particle state density. It is further assumed that if excited α -cluster is not emitted it interacts with other nucleons of the nucleus as four uncorrelated nucleons/33/.

The important point of the model is the so called preformation factor ϕ represent the probability that the preformed α -particle will be excited by the projectile. They applied this model to analyse a large number of $(\text{nucleon}, \alpha)$ reactions to extract the values of ϕ . Essentially the model contains two parameters: the single particle state density for α -particles and their preformation probability. More precisely, the probability for a nucleon to interact with an α -particle instead of interaction with a nucleon is adjusted. Both model parameters raised questions and doubts to the model formulation. The data analysis yielded preformation parameters upto 80% for nuclei in the rare earth region and 20% for gold. These values were thought to be too large/34/. More criticism was due to the applied single-particle state density, $g_\alpha = g/4$. For a nucleon quartet, Oblozinsky and Ribansky /35/



proposed $1/g_{\alpha} = 2/g_{\pi} + 2g_{\nu} = 8/g$. Later model formulations of Gadioli et al /36/ employed $g_{\alpha} = A/10$ MeV. The data analyzed by Millazzo, Colla and Braga Marcazzan /32/ were restricted to only low bombarding energies where the first interaction exhausts nearly all of the cross section. The model was extended by Gadioli et al. /36/ to have all quantities necessary to treat multistep processes. Analysis of (p, α) reactions upto higher energies yielded preformation probabilities of < 0.1 which are decreasing with bombarding energy.

(b) Coalescence Model :

This model, originally proposed by Blann and Lanzafame /37/, was later developed by Cline /38/ in an attempt to analyse the spectra of d, t, ^3He , and α particles from several nuclear reactions using a modified Exciton model formulation. Cline derived the following expression for the emission rate of complex particles

$$W_{\beta}(n, \epsilon_{\beta}) d\epsilon_{\beta} = (2S_{\beta} + 1) \frac{m_{\beta} \epsilon_{\beta}}{\pi^2 \hbar^3} \sigma_{\text{inv}}(\epsilon_{\beta}) \left[\frac{\rho(p - p_{\beta}, h, U)}{\rho(p, h, E)} \right] R_{\beta}(p) p_{\beta}^{-1} d\epsilon_{\beta} \quad (69)$$

where $n=p+h$, is the exciton number of the composite nucleus, s_{β} is the spin, m_{β} and ϵ_{β} are the reduced mass and energy of the complex particle β , σ_{inv} is the inverse cross section and ρ is the state density and U and E are the excitation energies of the residual and composite nuclei. The new parameter, $R_{\beta}(p)$ represents the probability that a group of p_{β} particles, chosen at random out of the total number of p excited particles, has the right combination of numbers of protons and neutrons to form the outgoing particle. p_{β} is an empirical constant found necessary to reproduce the relative yields of different particle types. The model is called 'Coalescence Model'. With the above assumptions, for each reaction system, the model parameters

were adjusted to reproduce the proton spectrum and the spectra for the remaining four particle types were calculated with no additional adjustable parameters. However, no term representing the physical probability of the formation of the specific particle was introduced, as $R_{\beta}(p)$ represents only the purely combinatorial probability of the formation process, and also, on the contrary, it was necessary to increase the decay rate by the factor p_{β} was experimentally determined to bring calculated yields for the reaction system $^{54}\text{Fe}+62\text{MeV}$ protons into the same order of magnitude as experimental ones. However, data for heavier nuclei were less reproduced. It was pointed out by Ribansky and Oblozinsky /39/ that not only in the residual system, there are a lot of possibilities for the excitons form a cluster. They, therefore, replaced $p_{\beta!}$ by $\left[\frac{\rho(p_{\beta}, 0, E - U)}{g} \right] \gamma_{\beta}$ where the term in the square bracket represents the distinguishable configuration of p_{β} nucleons from which the complex particle β can be formed in the composite nucleus with the average probability γ_{β} . The new model, parameter γ_{β} , is the fraction of all possible states where p_{β} nucleons have the right spin and isospin to form a cluster of type β . The energy dependence in the above factor led to better agreement in the spectral shapes between data and calculation. The model parameter γ_{β} was always adjusted to fit the data. However, it was not compared with calculated values nor could it be reduced to other physical quantities.

(c) The Exciton Coalescence Model :

The Exciton Coalescence model is developed by Machner /40/ to overcome the shortcomings of the Coalescence model. It is a combination of the Coalescence model of Butler and Pearson /41/ and the aspects of the Generalized Exciton model. The basic idea is that only those nucleons coalesce which have small relative

momenta, i.e. which nearly fly parallel having the same velocity. Then the direction of a cluster is just the direction of the leading particle having momentum P_c , which picks up other nucleons. If one assumes that p_β nucleons having relative momenta smaller than a momentum P_0 coalesce to form a cluster β , then the probability of forming a cluster appearing as the complex emitted particle β , is just the probability of finding p_β nucleons, including the leading particle, within a sphere of radius P_0 around the momentum P_c , in momentum space. Incorporating these ideas into Master Equation approach of the Exciton model, Machner developed the Exciton Coalescence model and compared its predictions with experimental data on the α -emission from the composite system ^{65}Zn /42/ at an exciton energy of 37.4 MeV which is formed in a Ghosal type of experiment /43/. The intermediate system ^{65}Zn was produced via three different entrance channels $^{63}\text{Cu} + d$; $^{62}\text{Ni} + ^3\text{He}$ and $^{61}\text{Ni} + \alpha$. Machner derived the radius of the coalescence sphere, P_0 , for each case from the data. The radii of the coalescence sphere have been treated as free parameters and are derived by fitting the angle integrated spectra. From the analysis it turned out that in cases where projectile and ejectile are same type of particles the radii P_0 are larger than in other cases. This is evidence that already in the entrance channel there are correlated nucleons which may be emitted with high probability after interaction with target nucleons. Larger P_0 values mean, under the assumptions of phase space relations, a smaller volume in the nucleus from which the particle is being emitted. Therefore, a possible explanation of large P_0 values may be that at least a part of the projectile particle survives nucleon interactions. There have been many other models /44/ which discuss the complex particle emission in a greater detail. The sizes of the model parameters are open questions in all these models.; However, the model parameters are not independent of each other. As an example, pre-formation probability and single particle state density influence the absolute cross sections. The same is true for the depth of the potential wells in the quasi-free

scattering model /44/. This means in conclusion that model parameters obtained from data analysis are not unique.

II. 2.8 Quantum Mechanical Theory :

Most of the preequilibrium models described above are basically semi-classical or phenomenological models, lacking in quantum theoretical foundations. To make up for this, Feshbach, Kerman and Koonin /45/ proposed a quantum statistical theory known as multistep compound and multistep direct reaction theory.

Multistep Direct and Multistep Compound Reaction Theory

A fully quantum-mechanical theory of preequilibrium emission was developed by Feshbach, Kerman and Koonin /45/ in 1980. Like the Exciton model theories described in the previous section, it considers the excitation process to take place in a number of stages. At each stage a distinction is made between the states with atleast one particle in the continuum and the states with all particles bound, and these are formally described by the projections P and Q acting on the total wavefunction ψ , with $P+Q = 1$. This enables the multistep process to be divided into two physically different types of reaction : the multistep direct (MSD) reactions described by the states $P\psi$ and the multistep compound (MSC) reactions described by the states $Q\psi$.

The division of the excitation process into these two types of reaction is shown in figure II.3 with dashes indicating the transitions from one configuration to another. If only two-body interactions contribute, these transitions can only take place between neighbouring states; this is the so-called chaining hypothesis. As in the exciton model, transitions to states of greater complexity are such more probable

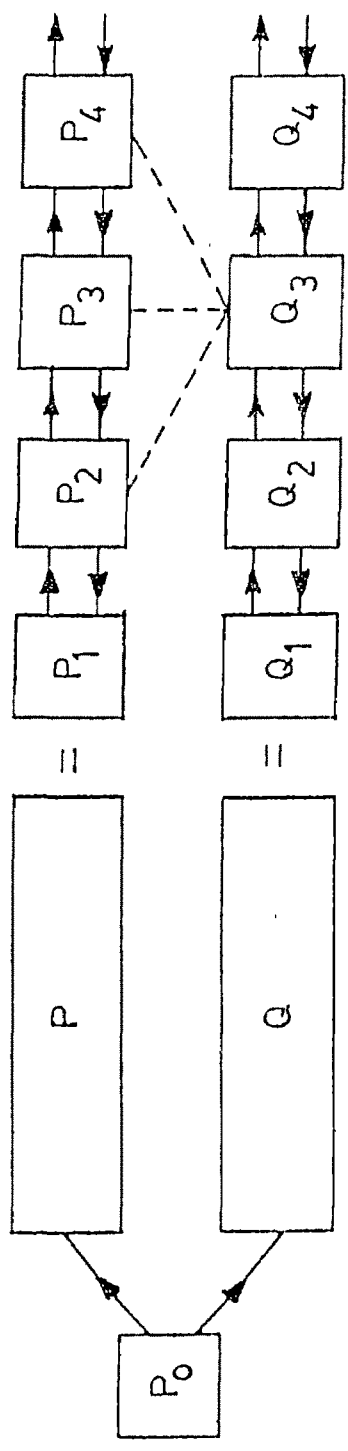


Fig.II.3 MULTI-STEP DISCRPTION OF A NUCLEAR REACTION

than transitions to states of lesser complexity. Pre-equilibrium emission can take place directly from each stage in the P chain, or indirectly from the Q chain in three different ways as shown in figure II.3.

The proportion of the reaction going down the P and Q chains depends strongly on the incident energy. At low energies the Q chain interactions dominate, giving multistep compound emission. As the energy increases the P chain interactions become increasingly important until finally they are responsible for most of the cross-section, giving forward peaked multistep direct emission. The transitions between the P and Q chains are small and average out, so that the cross-sections attributable to the P and Q chains can be evaluated separately, and their sum compared with experiment.

The P-chain transitions take place rapidly and the preequilibrium particles retain some memory of the direction of the projectile, giving forward peaked angular distributions. The Q chain transitions take place much more slowly at each stage there are many interactions that exchange energy but do not alter the exciton number. A quasi-equilibrium is established, giving an angular distribution that is symmetric about 90° , but with a life time that is shorter and temperature that is higher than that of the fully-equilibrated compound nucleus.

The cross section of the multistep compound process has the form

$$\sigma_{PE} = \sigma_c \sum_{n=1}^N \frac{\Gamma^\uparrow \rho_f}{\Gamma} \prod_{i=1}^n \left(\frac{\Gamma^\downarrow}{\Gamma} \right) \quad (70)$$

where Γ^\uparrow is the escape width for preequilibrium emission and Γ^\downarrow is the damping width for a transition for the (n-1)th to the nth stage. The total width $\Gamma = \Gamma^\uparrow + \Gamma^\downarrow$,

and ρ_f is the density of states in the final nucleus, when the reaction goes to the continuum.

The density of particle-hole states is given by the formula of Ericson /7/

$$\rho_{p,h}(E) = \frac{g^n E^{n-1}}{p!h!(n-1)!} \quad (71)$$

where E is the excitation energy, g the single particle level density and p, h the numbers of particles and holes, and $n = p+h$.

The final state density is then given as a product of energy dependent and J-dependent factors

$$\rho_f(E, J) = \rho_{ph}(E) \frac{2J+1}{2\sqrt{2\pi}\sigma^{3n}} \exp\left[-\frac{(J+1/2)^2}{2\sigma^2}\right] \quad (72)$$

where $\sigma^2 \cong 0.28 MA^{2/3}$ is the spin cut-off parameter.

The cross section σ_i , for the formation of the compound nucleus is calculated from the optical model and the damping and escape widths are the product of three factors

$$\Gamma = 2\pi I XY \quad (73)$$

where I is the interaction matrix element, X contains the angular momentum coupling coefficients and Y is a statistical factor.

The interaction matrix element is given by

$$I = \int u_1(r) u_2(r) V(r) u_3(r) u_4(r) dr \quad (74)$$

where the $u(r)$ are the radial wavefunctions of the interacting nucleons and $V(r)$ is the effective interaction. The matrix element corresponding to the damping width refers to the interaction of two nucleons labelled 1 and 2 that result in the formation

of an additional particle-hole pair. These are two ways in which this can take place. The matrix element corresponding to the escape width refers to a similar interaction that results in two nucleons, one of which is a particle with sufficient energy to escape from the nucleus. There are four such processes and they may or may not change the number of particle hole pairs. The three possibilities, changing the number of particle-hole pairs by -1 , 0 or $+1$, correspond to the three dashed lines from the Q chain to the P chain. The radial wavefunctions $u(r)$ can be calculated from the harmonic oscillator model for bound nucleons and from the optical model potential for particles that escape.

The effective interaction $V(r)$ is the product of a strength and a radial form factor.

$$V(r) = V_0 f(r) \tag{75}$$

and it is usual to take $f(r)$ as a delta function, which greatly simplifies the calculations. The more realistic Yukawa form $\exp(-\mu r)/r$ gives nearly the same results, provided the strength V_0 is appropriately adjusted. This strength is an adjustable parameter in the theory but in cases where the cross-sections, in all open channels, are known it may be determined by the requirement that the total reaction cross-section is that given by the optical model.

At higher energies it is increasingly likely that throughout the reaction there is always at least one particle in the continuum. In these cases the reaction proceeds by the multistep direct process represented by the P chain in figure II.3. The multistep compound and multistep direct processes add incoherently so in the energy range where both contribute, it is sufficient to calculate the corresponding cross-sections separately and add these for comparison with the experimental data.

The total cross section for the multistep direct emission is the sum of the emissions from all stages of the P chain

$$\frac{d^2\sigma}{d\Omega d\varepsilon} = \frac{d^2\sigma}{d\Omega d\varepsilon_{\text{onestep}}} + \frac{d^2\sigma}{d\Omega d\varepsilon_{\text{multistep}}} \quad (76)$$

Defining $W_{N, N-1}$ as the probability for the transition from the (N-1) th to the Nth stage the total multistep cross section becomes

$$S_{\text{multistep}} = \sum_N S_N \sum_{M=N-1}^{N+1} W_{MN} W_{N, N-1} \dots W_{21} S_1 \quad (77)$$

where S_N is the emission cross section from the Nth stage, when this expression is evaluated it is integrated overall intermediate angles and momenta.

This transition matrix element

$$W_{N, N-1} = 2\pi^2 \rho(K_N) \rho_N(U) \langle V_{N, N-1}(K_N, K_{N-1})^2 \rangle \quad (78)$$

where $\rho(K_N) = mK/(2\pi)^3 v^2$ is the density of particle states in the continuum $\rho_N(U)$ the level density of the residual nucleus at excitation energy U and $v_{N, N-1}(K_N, K_{N-1})$ is the matrix element describing the transition from a state N-1 to a state N when the particle in the continuum changes its momentum from K_{N-1} to K_N . This matrix element is given by the distorted wave Born approximation expression

$$U_{a,b}(K_i, K_f) = \int x_a^{(-)*} \langle \psi_i | V(\mathbf{r}) | \psi_f \rangle x_b^{(+)} d\mathbf{r} \quad (79)$$

where $V(\mathbf{r})$ is the effective interaction for the transition, $x_a^{(-)}$ and $x_b^{(+)}$ the incoming and outgoing distorted waves and ψ_i and ψ_f the initial and final nuclear states.

In the expression for the transition matrix elements, the transition probability is averaged over many final states so that the interference terms cancel and the orbital angular momenta contribute incoherently. The averaged value of the squared matrix element then becomes

$$\langle |V(K_i, K_f)|^2 \rangle = \sum_L \langle |V_L(K_i, K_f)|^2 \rangle S_N^2 \quad (80)$$

where S_N^2 is the spin distribution function of the residual nucleus.

The comparison between experiment and theory mode so far indicate that the essential physics of these multistep reactions is now quite well understood, but there still remains much work to be done to verify the theory over a wider range of energies and target nuclei and to determine its parameters more precisely. It is also desirable to include in the theory the emission of composite particles like neutrons and α -particles and to extend it to incident composite particles. One of the major sources of uncertainty in the calculation at present is lack of knowledge of the compound state and final state level densities.

II.2.9 Preequilibrium Angular Distributions :

The preequilibrium models discussed so far deal with angle integrated parameters and are therefore incapable of describing angular distribution. The first calculations of preequilibrium angular distributions were performed with intranuclear cascade model using the concept of quasi-free scattering inside the nucleus - a concept valid for energies greater than 100 MeV but used nevertheless for reactions induced by projectiles with energies of a few tens of MeV. The two most widely used models of precompound angle integrated energy spectra viz. the Exciton model and the Hybrid models have also been extended to obtain angular distributions. Angle dependent transition rates are introduced in the Master Equation of the Exciton model to describe both ejectile energy and angle distributions. The kinematics of multiple two-body scattering is used in the frame work of the Hybrid model to introduce angle dependence in the preequilibrium emission probabilities. These models are described in the following.

(a) Intranuclear Cascade Model :

The idea of nuclear relaxation by two-body collisions was first suggested by Serber /1/ in 1947 to explain the high energy interactions between nucleons and nuclei. He pointed out that when incident nucleon wavelengths were short relative to internucleon distances within the nucleus (e.g. for incident nucleon energies in excess of 100 MeV), the interaction could be treated as a quasi-free scattering process where the target nucleus is taken to be a Fermi gas. In this approach, the mean free paths and energy transfers are based on nucleon-nucleon experimental scattering cross sections and angular distributions; collision between two particles with energy less than the Fermi energy are forbidden by the Pauli principle.

The intranuclear cascade model /19,46,47/ uses the Monte-Carlo method to simulate the interaction of the incident nucleon with those in the nucleus. The projectile is assumed to enter into the nucleus at a random impact parameter b . The distance of travel before a collision occurs is also chosen randomly, but is weighted to produce the mean free path determined from the nuclear density distribution and free nucleon-nucleon cross sections. At each collision site a scattering angle is randomly chosen from free nucleon-nucleon angular distributions and the energy and direction of both nucleons are calculated. If the energy of either is below the Fermi energy the collision is forbidden by the Pauli exclusion principle and a new distance of travel is chosen. If the collision is not forbidden, the passage of both nucleons is followed in the manner described above until (1) the nucleon escapes from the nucleus or (2) it is scattered with energy below a pre-set cut-off value, typically ranging from 10 to 20 MeV. After all particles of a given cascade have met the eventualities mentioned in (1) or (2) above, the identity of the residual nucleus, its energy, recoil and angular momentum as well as the energies and directions of

emitted particles are recorded and a new cascade is initiated. The process is repeated until adequate statistics are obtained.

Residual nuclei from the cascade calculation are used as input for evaporation calculations. The number of particles sharing the residual energy may be quite small, depending on the cut-off energy used, which is contrary to the assumption of equilibrium. The actual attainment of equilibrium is not treated explicitly, but its effects are probability minimal.

Despite its early inception, the cascade model was not the first to be used to analyse results of preequilibrium reactions. Assumption of successive quasi-free scattering, using free nucleon-nucleon cross section, corrected by Pauli exclusion principle, was expected to be valid only when the wavelength of the incident nucleon was small compared to the mean distance between the nucleons in the nucleus. This criterion is met only above ~ 100 MeV/nucleon incident energy. Nevertheless, the model has been successful to some extent in predicting angular distribution and energy spectra of emitted proton in low energy reactions like $^{54}\text{Fe}(p,p')$ at 39 and 62 MeV bombarding energy /48/.

(b) Angular Distribution from the Master Equation :

The basic idea behind the angular distribution calculation in the Exciton model /49,50/ is the distinction between the “fast particle “ and the rest of the nuclear system. The “fast particle” i.e., the projectile , loses its energy and momentum (which contains the memory of the incident direction) in a cascade of two-body interactions. The “fast particle” remains “fast”, i.e., retains its energy of incident momentum only in a fraction of the two-body interactions needed to reach

the compound nuclear steady state configuration. It is this fraction, however, that gives rise to the forward peaking of the angular distributions.

Mantzouranis et al /49/ generalised the Master Equation of the Exciton model to include an angle dependent part in the transition rates. The exciton states are labelled by (n, Ω) , the exciton number and the direction Ω of the “fast particle” in the laboratory frame. Defining $\lambda_+^n (\Omega' \rightarrow \Omega)$ and $\lambda_-^n (\Omega' \rightarrow \Omega)$ as transition rates from (n, Ω') to $(n+2, \Omega)$ and $(n-2, \Omega)$, respectively, the occupation probability $P_n(\Omega, t)$ of the state (n, Ω) at time t is written as

$$\begin{aligned} \frac{d}{dt} P_n(\Omega, t) = & \int \lambda_+^{n-2}(\Omega' \rightarrow \Omega) P_{n-2}(\Omega', t) d\Omega' + \int \lambda_-^{n+2}(\Omega' \rightarrow \Omega) P_{n+2}(\Omega', t) d\Omega' \\ & - \int \lambda_+^n(\Omega' \rightarrow \Omega) P_n(\Omega, t) d\Omega' - \int \lambda_-^n(\Omega' \rightarrow \Omega) P_n(\Omega, t) d\Omega' \\ & - P_n(\Omega, t) \sum \int \lambda_c^n(\varepsilon) d\varepsilon \end{aligned} \quad (81)$$

As in eqn.(34) the first two terms give the growth of the state (n, Ω) and the last three terms give its decay rate.

The angle dependent transition rates are factorised into the usual angle independent transition rate and an angle dependent part

$$\begin{aligned} \lambda_+^n (\Omega' \rightarrow \Omega) &= \lambda_+^n G(\Omega' \rightarrow \Omega) \\ \lambda_-^n (\Omega' \rightarrow \Omega) &= \lambda_-^n G(\Omega' \rightarrow \Omega) \end{aligned} \quad (82)$$

Assuming $G(\Omega' \rightarrow \Omega)$ to be proportional to the free nucleon-nucleon scattering cross section, one obtains

$$G(\Omega' \rightarrow \Omega) = \frac{d\sigma^f}{d\Omega} / \int \frac{d\sigma^f}{d\Omega} d\Omega \quad (83)$$

where $d\sigma^f / d\Omega$ is the free nucleon-nucleon differential scattering cross section. This cross section is isotropic in the centre of mass frame of the interacting nucleons and hence

$$G(\Omega_c \rightarrow \Omega_c') = G(\Omega_c' \rightarrow \Omega_c) = \frac{1}{4\pi} \quad (84)$$

where Ω_c, Ω_c' are the directions in the centre of mass frame of the two nucleons

$$\text{and } G(\Omega \rightarrow \Omega') = G(\Omega' \rightarrow \Omega) = G(\Omega_c \rightarrow \Omega_c') \frac{d\Omega_c}{d\Omega} \quad (85)$$

If the Fermi motion of the target nucleons is neglected then

$$d\Omega_c / d\Omega = 4 \cos\theta \cdot H(\pi/2 - \theta) \text{ and } G(\Omega \rightarrow \Omega') = \frac{1}{\pi} \cos\theta \cdot H\left(\frac{\pi}{2} - \theta\right) \quad (86)$$

where θ is the laboratory angle and $H(x)$ is the Heaviside step function. The initial condition for solving eqn.(81) is

$$P_n(\Omega, t) = \delta_{nn_0} \pi^{-1} \cos\theta H(\pi/2 - \theta) \quad (87)$$

It is to be noted that three different reference frames come into the picture. First there is the centre of mass frame of interacting nucleons in which $d\sigma^f/d\Omega$ is isotropic. The directions in this frame are denoted by the subscript c. Second, there is the laboratory frame in which the directions carry no superscript or subscript. Third, there is the centre of mass of the projectile and the target which has not been used so far. If calculations are to be performed in this third frame then eqn.(85) is to be multiplied by the Jacobian corresponding to the transformation from the laboratory to the centre of mass frame of the projectile and the target.

(c) Multiple Two - Body Scattering Kinematics:

The preequilibrium cross section for the emission of a nucleon of type ν can be written as

$$\frac{d^2\sigma}{d\varepsilon d\Omega} = \sigma_{obs} \sum_N {}_N P_v(\varepsilon, \Omega) d\varepsilon d\Omega$$

$$\frac{d^2\sigma}{d\varepsilon d\Omega} = \sigma_{obs} \sum_N F_N f_v P_N(\varepsilon, \Omega) \left[\frac{\lambda_c(\varepsilon)}{\lambda_+(\varepsilon) + \lambda_c(\varepsilon)} \right] \quad (88)$$

where ${}_N P_v(\varepsilon, \Omega) d\varepsilon d\Omega$ is the emission probability of a particle of type v after N two body interaction with energy between ε and $\varepsilon+d\varepsilon$ in the direction between the solid angles Ω and $\Omega+d\Omega$. $P_N(E, \Omega)$ is the probability that after N binary interactions a particle moves in the direction Ω with the energy E inside the nucleus.

Eqn.(88) is a reformulation of the Hybrid model. When integrated overall emission angles it reduces to the hybrid model eqn. (46) for the angle integrated energy spectrum. In writing eqn. (88) the Hybrid model has been reformulated in the following respects. First ejectile emissions are considered after each two-body interaction instead of from a given n -exciton state as is done in the hybrid model. Secondly, $P_N(E, \Omega)$ and consequently the probability $P_N(E) = \int d\Omega P_N(E, \Omega)$ is obtained from the kinematics of multiple nucleon-nucleon scattering. While the corresponding Hybrid model probability of a nucleon having energy ε in the n -exciton state is expressed as the ratio of the final to the initial partial level densities.

To obtain $P_N(E, \Omega)$ from nucleon-nucleon scattering kinematics we use, for convenience $P_N(E, \Omega) dE d\Omega \equiv P(k) dk$, the probability of a particle having momentum between k and $k+dk$, after N two-body interactions. After the first two-body interaction between the projectile and the target nucleon with momentum k_1 , the probability that one of the scattered particles has momentum k is $P_{N=1}(k) = P(k_1 \rightarrow k)$, the transition probability from initial momentum k_1 to final momentum k , k_1 being the projectile momentum inside the nucleus.

The differential cross section $\sigma(k_1 \rightarrow k)dk$ for this transition is given by

$$\sigma(k_1 \rightarrow k)dk = \int_{k_i} \frac{2k_r}{k} \sigma(k_r, k'_r) \frac{d\Omega'}{dk} dk P(k_i) dk_i \quad (89)$$

where k_r and k'_r are the relative momenta of the nucleons before and after scattering respectively. $\sigma(k_r, k'_r)$ is the scattering cross section in the centre of mass frame of the interacting nucleons, while k_1 , k and k_i are in the laboratory frame. k_r and k'_r are the same in the two frames. If $d\Omega'/dk$ is expressed as a function of k_r and k'_r , then $\sigma(k_r, k'_r) (d\Omega'/dk)$ becomes invariant in the two reference frames and can be solved in the laboratory frame /20/ after necessary algebra.

$$\sigma(k_1 \rightarrow k)dk = \frac{4dk}{k_1} \int \delta(k_r'^2 - k_r^2) \sigma(k_r, k'_r) P(k_i) dk_i \quad (90)$$

where δ function ensures energy and momentum conservation. Since the transition probability $P(k_1 \rightarrow k)dk$ is proportional to the cross section $\sigma(k_1 \rightarrow k)dk$ eqn.(90) become

$$P(k_1 \rightarrow k)dk = \frac{4dk}{k_1} \int \delta(k_r'^2 - k_r^2) P(k_r, k'_r) P(k_i) dk_i \quad (91)$$

where $P(k_r, k'_r)$ is the transition probability from k_r to k'_r and corresponds to the nucleon - nucleon differential scattering cross section $\sigma(k_r, k'_r)$.

Once $P_{N=1}(k)$ is known $P_N(k)$ for all subsequent two-body interactions can be obtained from the recursion relation

$$P_N(k) = \int P_{N-1}(k') P(k' \rightarrow k) dk' \quad (92)$$

where the scattering kernel $P(k' \rightarrow k)$ is defined by eqn.(91) with k' replacing by k_1 .

The solutions of eqn.(91) have obtained by Kikuchi and Kawai/20/ as

$$P(k_1 \rightarrow k) = \frac{3P(k_1)}{4\pi k_1 k_f^3 q^3} \{k_1^2 k^2 \sin^2 \phi - q^2 (k^2 - k_f^2)\} \quad (93)$$

$$P(k_1 \rightarrow k) = \frac{3P(k_1)}{4\pi k_1 k_f^3 q} (k_1^2 - k^2) \quad (94)$$

where k_f is the Fermi momentum, ϕ is the scattering angle and q is the magnitude of the momentum transfer : $q^2 = k_1^2 + k^2 - 2k_1 k \cos\phi$.

Using the above solutions for $P(k_1 \rightarrow k)$ Chiang and Hufner /51/ have solved eqn.(88) to obtain the angular distribution of precompound emissions, however the back-angle cross sections are grossly under predicted.

(d) Multiple Two-body Scattering and Nuclear Excitation :

A possible reason for the failure of the semi-classical models to describe preequilibrium angular distribution, particularly at back angles could be the incorrect treatment of the motion of the target particles. The master equation calculations totally ignore nucleon motions. The nucleon motions are taken into account to evaluate the nucleon-nucleon scattering kinematics but it is assumed that throughout the relaxation process the nucleon momenta are described by the zero-temperature Fermi distribution; i.e., it is assumed that the excitation brought in by the projectile has negligible effect on the motion of the target particles.

At the time of the first two-body interaction the target nucleus is in the ground state and the nucleon motions may be approximated by a zero-temperature Fermi distribution. During the subsequent interactions the composite nucleus is excited and the zero-temperature Fermi distribution may be an inadequate approximation. The effect of the nuclear excitation on preequilibrium angular distribution has been investigated by De et al /52/ using a finite excitation Fermi distribution to describe $P(k)dk_1$:

$$P(k_i)dk_i = \frac{3dk_i}{4\pi k_i^3} \left[1 + \exp\left\{ \beta(k_i^2 - k\mu^2) / 2m \right\} \right] \quad (95)$$

where $k_\mu^2 = 2m\mu$, μ being the chemical potential and m the nucleon mass. The excitation parameter β is infinity for a ground state nucleus and has a finite value for an excited system. Analytic solutions of eqn.(91) with $P(k_i)dk_i$ of eqn.(95) have been obtained as a function of β /53/. β is uniquely defined at every stage of the binary cascade by the statistically weighted average of all possible configurations in that particular state /54/. $P_N(E, \Omega)$ are then calculated from the recursion relation eqn.(92) and finally the angular distribution obtained from eqn.(88). The order of magnitude discrepancies in the back-angle cross section calculations of semi classical models are removed, if not completely, at least substantially through the introduction of excitation effects.

II. 2.10 Important Improvements in Hybrid Model :

(a) Multiple Precompound Emission :

An important modification has been made by Blann and Vonach /28/ to account for multiple precompound decay, which was not included in earlier Hybrid model formulations, and which becomes significant at the higher excitation energies. Such refinements are necessary for determining the cross section surviving upto the stage of the compound nucleus, and in determining yields of products which are formed after multiparticle emission from the composite systems.

As earlier discussed, there are possibly two types of multiple precompound decay. Type I, accounts for the emission of more than one exciton from a single exciton hierarchy. It was observed that this mode of decay becomes important above

50 MeV of excitation energy. On the other hand the second type of precompound decay (Type II) is an extended version of Type I decay, in which after the emission of one particle, as in Type I, there are one or more two-body intranuclear transitions in the residual nucleus, followed by another particle emission. Because the first particle emission leaves a large number of residual excitations and exciton numbers, a calculation of Type II, emission becomes more complex and time consuming than for Type I emission. Thus Type I emission has been included in the latest version of the Hybrid model.

In their treatment of Type I emission, Blann and Vonach made the assumption that if P_n and P_p are the total number of neutron and proton excitons emitted from a particular exciton number configuration, then the number of either type of particle emitted in coincidence with the other from the same nucleus and exciton heirarchy is given by

$$P_{np} = P_{pn} = P_n P_p \quad (96)$$

Also the number of neutrons emitted in coincidence with another neutron from a particular exciton number configuration is given by

$$P_{nn} = 2 P_n / 2 P_n / 2 \quad (97)$$

Similar expressions are used for proton-proton coincidence emission.

The number of neutrons (protons) emitted from the n-exciton configuration which are not in coincidence with another particle is given by

$$\begin{aligned} P_n \text{ (n only)} &= P_n - P_{nn} - P_{np} \\ P_p \text{ (p only)} &= P_p - P_{pp} - P_{np} \end{aligned} \quad (98)$$

The fraction of the population F_n which had survived decay of the exciton number in question is

$$F_n = 1 - P_n \text{ (n only)} - P_p \text{ (p only)} - P_{pp}/2 P_{nn}/2 - P_{np} \quad (99)$$

This fraction would multiply the fractional population which had survived to the n -exciton state, giving the fraction of the original population which is available for decay from the $(n+2)$ exciton state. The treatment of multiple emission is completed by storing spectra of excited nuclei into the appropriate daughter nucleus buffers following the emission of one neutron only, one proton only, one neutron and one proton only, two neutrons only and two protons only. The sum of these cross sections plus the original compound nucleus cross section gives the reaction cross section. This aspect of the calculation is very effective on the excitation functions for those products, which involve the emission of one or two neutrons or protons in the precompound mode.

(b) Intranuclear Transition Rates :

The present model employs the Pauli corrected nucleon-nucleon scattering cross sections to evaluate the intranuclear transition rates as these are valid upto 200 MeV or more. Those evaluated from the imaginary optical potential (using parameters due to Becchetti and Greenless) are valid only for projectile energies below 55 MeV.

(c) Single Particle Level Density and Fermi Energy :

In the earlier version of Hybrid model, the Fermi energy (ϵ_F) has been taken as 40 MeV for saturation density, and is assumed to vary as the average density to the two-thirds power. The value of ϵ_F so evaluated is used in evaluating the single particle level density “ g ” for all calculations, as this should be the property of the average potential.

In this modified version of Hybrid model, the single particle level densities have been defined by,

$$g_n = \frac{N}{20} \left[\frac{\varepsilon_F + B_p + \varepsilon}{\varepsilon_F} \right] \quad (100a)$$

$$g_p = \frac{Z}{20} \left[\frac{\varepsilon_F + B_p + \varepsilon}{\varepsilon_F} \right] \quad (100b)$$

In this case a constant 20 is used, instead of 14 as used in the earlier versions of this model. Values of $g_n = N/14$ and $g_p = Z/14$ gave nearly identical spectra when used in place of the energy-dependent single particle level densities.

(d) Inverse Reaction Cross sections :

The code ALICE/85/300 /55/ based on this modified version of Hybrid model, uses a classical sharp-cut off routine to calculate inverse reaction cross sections upto 90 MeV, employing the earlier optical model parameters. The optical model routine in the earlier code ALICE used a pure surface form-factor-parameter set for nucleon induced reactions. This should be consistent with compound nucleus evaporation, but at higher energies (upto 90 MeV), where the precompound effects dominate, these parameters are not suitable.

Hybrid model code which combine precompound and compound decay channels have proven to be very successful in a wide range of projectile energies. One of the important inputs to these calculations is the nuclear level density as a function of the excitation energy .It has long been known that the yields of nuclides with closed or nearly closed nucleon shells are not predicted well when standard Fermi gas level densities are used in the “evaporation” phase of the de-excitation calculation . In such cases , Kataria et al /56/ incorporated a shell dependent level density formula due to Kataria, Ramamurthy and Kapoor /13/ into the code

ALICE/85/300 /55/. This version of the code is known ALICE/90. This model relates the shell effects in the nuclear level densities to the shell correction term of the nuclear mass surface. Because the ALICE code contains a library of experimental masses as well as a liquid drop mass formula /57/, the necessary shell correction terms can be generated internally, requiring no effort on the part of the user.

In the recent year Blann formulated a new precompound decay model which allows unlimited multiple precompound emission for each interaction may be used to give exclusive spectra and yields. The new approach is a Hybrid Monte Carlo Simulation model known as Alice-HMS code /58/. It should be valid upto the effective pion threshold , around 280 MeV and higher until pion production becomes a significant fraction of the inelastic nucleon-nucleon scattering cross section i.e., to around 400 MeV.

However in the present work we have used the code ALICE/90.

References :

- /1/ R.Serber, Phys.Rev. **72**,1114(1947).
- /2/ N.Austern, Direct Nuclear Reaction Theories (Wiley-Interscience, New York , 1965)
- /3/ N.Bohr, Nature **137**,344 (1936).
- /4/ V.F. Weisskopf, Phys. Rev. **52**, 295 (1937).
- /5/ H.A.Bethe, Revs. Mod. Phys. **9**, 69(1937)
- /6/ J.M.Blatt and V.F.Weisskopf "Theoretical Nuclear Physics", John wiley Inc. New Yourk (1952).
- /7/ T. Ericson, Advance in physics **9**, 425 (1960).
- /8/ V.F. Weisskopf and D.H. Ewing, Phys.Rev. **57**, 472 (1940).
- /9/ A.G. W. Cameron, Can. J. Phys. **36**, 1040 (1958).
- /10/ T.D. Newton, Can. J. Phys. **34**, 804 (1956).
- /11/ A.Gilbert and A.G.W. Cameron, Can.J.Phys. **43**,1446(1965).
- /12/ A.V.Ignatyuk, G.N.Smirenkin and A.S.Tishin, Sov.J. Nucl.Phys. **21**,255(1975).
- /13/ S.K.Kataria, V.S. Ramamurthy and S. Kapoor , Phys. Rev. **C18**, 549 (1978).
- /14/ J.J. Griffin, Phys. Rev. **17**,478 (1966).
- /15/ F.C. Williams Jr. Phys. Lett. **31B**, 184 (1970).
- /16/ W.Pauli, Festschrift Zum 60, Geburtstag Sommerfelds, Hirzel Verlag, Leipzig (1928)
- /17/ G.M.Braga-Marcazzan, E.Gadioli-Erba, L.Millazzo Colli and P.G.Sona, Phys. Rev. **C6**, 1398(1972).
- /18/ C. Kalbach and C.K. Cline, Nucl. Phys. **A210**, 590 (1973).
- /18a/ C. Kalbach Z. Phys. **A287**, 319 (1978).
- /19/ M.L. Goldberger, Phys. Rev. Lett. **74**,1269 (1948).

- /20/ K. Kikuchi and M.Kawai, Nuclear Matter and Nuclear Reactions, North-Holland Publishing Co., Amsterdam (1968).
- /21/ E. Gadioli, E. Gadioli-Erba and P.G. Sona, Nucl. Phys. **A217**, 589 (1973).
- /22/ F. D. Becchetti and G.W. Greenless, Phys. Rev. **182**, 1190 (1969).
- /23/ G.D. Harp, J. M. Miller and B.J. Berne, Phys. Rev. **165**, 1166 (1968).
- /24/ G.D. Harp and J. M. Miller, Phys.Rev. **C3**,1847(1971).
- /25/ M. Blann, Phys. Rev. Lett. **27**, 337 (1971).
- /26/ M.Blann, Ann.Rev.Nucl.Sci. **25**,123 (1975).
- /27/ M. Blann, Phys. Rev. Lett. **28**, 757 (1972).
- /28/ M. Blann and H.K. Vonach, Phys. Rev. **C28** , 1475 (1983).
- /29/ E.Gadioli, E.Gadioli-Erba, G.Tagliaferri and J.J.Hogan, Phys.Lett. **65B**, 311(1976).
- /29a/ M.Blann, Phys.Lett. **67B**,145(1977).
M.Blann, Phys.Rev. **C17**,1371(1978).
- /30/ J.Ernst and J. Rama Rao, Z. Phys. **A281**, 129 (1977).
- /31/ J.Bisplinghoff, Phys. Rev. **C33**, 1570 (1986).
- /32/ L. Millazzo Colli and G.M. Braga-Marcazzan, Phys. Lett. **38B** , 155 (1972)
Nucl.Phys.**A210**, 297(1973).
- /33/ E.Gadioli, E. Gadioli - Erba and J.J.Hogan, Phys.Rev. **C16**,1404(1977).
- /34/ N.Cindro, In: E.Sheldon edn., Int.Conf. on Interaction of Neutrons with nuclei, Univ. of Lowell, Mass 347(1976).
- /35/ P.oblozinsky and I.Ribansky, Phys.Lett.**74B**, 6(1978).
- /36/ E.Gadioli, E.Gadioli - Erba, I.Iori and L.Zetta , J.Phys.**G6**, 1391(1980).
- /37/ M.Blann and F. M. Lanzafame, Nucl.Phys. **A142**, 559 (1970).
- /38/ C.K.Cline, Nucl.Phys. **A193**, 417(1972).
- /39/ I.Ribansky and P.Oblozinski, Phys.Lett. **45B**, 318 (1973).
- /40/ H. Machner, Phys. Lett. **86B**, 129 (1979) : Phys.Rep. **127**, 309 (1985).

- /41/ S.T. Butler and C.A. Pearson, Phys. Lett. **1**,77 (1962).
- /42/ H.Machner, Phys.Rev. **21**, 2695 (1980).
- /43/ S.N.Ghosal, Phys.Rev. **80**,939 (1950).
- /44/ A.Mignerey, M.Blann and W.Scobel, Nucl.Phys. **A217**,125(1976).
W.Scobel, M.Blann and A .Mignerey, Nucl.Phys.**A287**, 301(1977).
- /45/ H. Feshbach , A.Kerman and S. Koonin, Ann.Phys. **125**, 929 (1980).
- /46/ N.Metropolis, R.Bivins, M.Storm, A.Turkevich, J.M.Milller and
G.Friedlander, Phys.Rev. **110**, 185&204 (1958).
- /47/ K.Chen, G.Friedlander and J.M.Miller , Phys.Rev. **176**, 1208(1968).
- /48/ H.W.Bertini, G.D.Harp and F. E.Bertrand, Phys.Rev. **C10**, 2472 (1974).
- /49/ G. Mantzouranis, D. Agassi and H.A. Weidenmuller,
Phys. Lett. **57B**, 220 (1975).
Z.Phys.**A276**, 145 (1976).
- /50/ J.M.Akkermans , H.Gruppelaar and G.Reffo , Phys.Rev. **C22**,73 (1980).
J.M.Akkermans, Phys.Lett. **82B**, 20 (1979).
- /51/ N.C.Chiang and J.Hufner, Nucl.Phys.**A349**,466(1980).
- /52/ A.De, S. Ray and S.K.Ghosh, J.Phys.**G11**, L79(1985).
- /53/ A.De, S. Ray and S.K.Ghosh, J.Phys.**G13**, 1047(1987).
- /54/ A.De, S. Ray and S.K.Ghosh, Phys. Rev. **C37**, 2441(1988).
- /55/ M.Blann, Code ALICE/85/300, Lawrence Livermore National Laboratory,
Report UCID– 20169 (1984), unpublished.
- /56/ S.K. Kataria , V.S. Ramamurthy , M. Blann and T.T. Komoto, Nucl.Inst. &
Meth. **A288**, 585(1990)
- /57/ W.D.Myers and W.J.Swiatecki, Ark. Fys. **36**, 343(1967).
- /58/ M. Blann , Phys. Rev. **C54**, 1341 (1996).